IOP Conf. Series: Materials Science and Engineering **121** (2016) 012023 doi:10.1088/1757-899X/121/1/012023

CO_2 storage in heterogeneous aquifer: A study on the effect of injection rate and $CaCO_3$ concentration

A Raza[1*], R Rezaee[2], C H Bing[1], R Gholami[1], R Nagarajan[1] and M A Hamid[1]

[1] Faculty of Engineering and Science, Curtin University, Miri, Sarawak, Malaysia
[2] Faculty of Science and Engineering, Curtin University, Bentley WA 6102, Australia

*Email: arshadraza212@gmail.com

Abstract. Trapping mechanisms taken place during and after CO_2 injection in a geologic storage medium are impacted by a number of parameters including injection rates together with rock and pore fluid compositions. There have been many studies on the factors controlling the capillary trapping and injectivity of CO_2 storage sites. However, there are only few works carried out discussing on the effect of flow rate and rock and fluids compositions in controlling the trapping mechanisms. In this paper a CO_2 storage site located in a heterogeneous aquifer is simulated to investigate the efficiency of structural, capillary and dissolution trappings as a function of injection rate and concentration of calcium carbonate. The results obtained from numerical analysis indicated that CO_2 injection must be made within an optimum injection rate for having an effective storage in place. It was also found that concentration of $CaCO_3$ is an important parameter to consider during the analysis as it drastically controls the fate of trapping mechanisms at high injection rates.

1. Introduction

CO_2 behaves as a supercritical fluid in storage mediums located at a depth of greater than 800 meters [1]. Aquifers located at 1-3 km below the surface are permeable geologic layers saturated with saline water, and confined with a caprock [2]. Due to its geological setting and high storage capacity, aquifer is probably one the best places for CO_2 storage [2, 3].

The major concern of Carbon Capture and Sequestration (CCS) technology is to ensure that CO_2 remains confined [4, 5] when efficient trapping mechanisms immobilize it in the storage site. Trapping of injected CO_2 into a saline aquifer, however, is done through a series of events including immobilization of CO_2 by structural features or capillary forces, dissolution, and chemical reactions of CO_2 with brine compositions and rock minerals [6]. These mechanisms are classified as structural [3, 7-9], residual [2, 8, 10], dissolution [8, 11, 12] or mineral [7-9] trappings which may take place in a saline aquifer medium. The relative contribution of these mechanisms, however, depends mainly on a number of parameters. For instance, residual trapping is a function of pore fluids and rock properties as well as injection rate, and reservoir conditions [13]. Dissolution trapping is sensitive to variation of pH and concentration of different ions in pore fluid [14]. The fate of the mineral trapping, on the other hand, depends mainly on the pressure, temperature, pH, geochemical conditions, and activity of the cations dissolved in water [12]. There are, however, few studies carried out in recent years discussing the impact of these crucial parameters on different trapping mechanisms [15-19].

The aim of this paper is to evaluate the effect of injection rate and concentration of $CaCO_3$ on the structural, residual and dissolution trapping mechanisms of heterogeneous aquifer. A numerical simulation is run through Eclipse software for the purpose of this study and efficiency of trapping mechanisms are evaluated and compared as a function of injection rate and $CaCO_3$ concentration.

Content from this work may be used under the terms of the Creative Commons Attribution 3.0 licence. Any further distribution of this work must maintain attribution to the author(s) and the title of the work, journal citation and DOI.
Published under licence by IOP Publishing Ltd

2. Simulation approach

In this study, CO_2 storage in an aquifer is exercised using Eclipse Reservoir Simulator to explore the interaction of structural, residual and dissolution trappings in the storage site. It is assumed that dissolution occurs instantly and gas-rich CO_2 is in equilibrium with water under isothermal conditions of 90ºC.

The dimension of the aquifer was 180 m × 180 m with a thickness of 15 m. The rock properties (i.e., porosity and permeability) of five layers of fluvial sand and shale were considered in the model. Figure 1 shows the heterogeneity level of the model in term of horizontal permeability. The model was brought to static equilibrium by considering an initial aquifer pressure of 300 bar at a depth of 2500 m. The model was 100% water saturated without any dissolved gas at the beginning of the simulation. The three prime directions of the model were uniformly meshed by 19 cells in the x-direction, 28 cells in the y-direction and 5 cells in the z-direction. The data set of input parameters used for static modeling of aquifer is listed in table 1.

An injection well was taken into account in the center of the aquifer at a depth of 2400 meter, where only resident brine and CO_2 are interacting in pore spaces. Pure CO_2 was injected for 35 years into the aquifer which appears as a supercritical fluid under injection conditions. No shut-in period was set in the simulation for creation of a driving force due to differential density. Along CO_2 and H_2O, the salt components NaCl, $CaCl_2$ and $CaCO_3$ were considered which can be present in both the aqueous phase and the solid phase during precipitation process. Different schemes were analyzed, aiming to find the effect of flow rate and $CaCO_3$ concentration on the trapping mechanisms. Table 2 presents an overview of simulation cases included in the numerical simulation. H_2O with 0.90 mole fractions and CO_2 with 0 mole fraction were adapted for three cases as given in table 3.

Fluid properties such as gas and brine densities (effect of salt and CO_2) were determined through utilization of equations of state and Ezrokhi's methods [20]. Molecular diffusion was introduced at the beginning of injection for creation of diffusive flow in terms of liquid mole fraction between grids and minimizing the interaction with the formation water. Relative permeability data of Viking sandstone was used for modeling purposes. Figure 2 displays the relative permeability functions considered through the simulation.

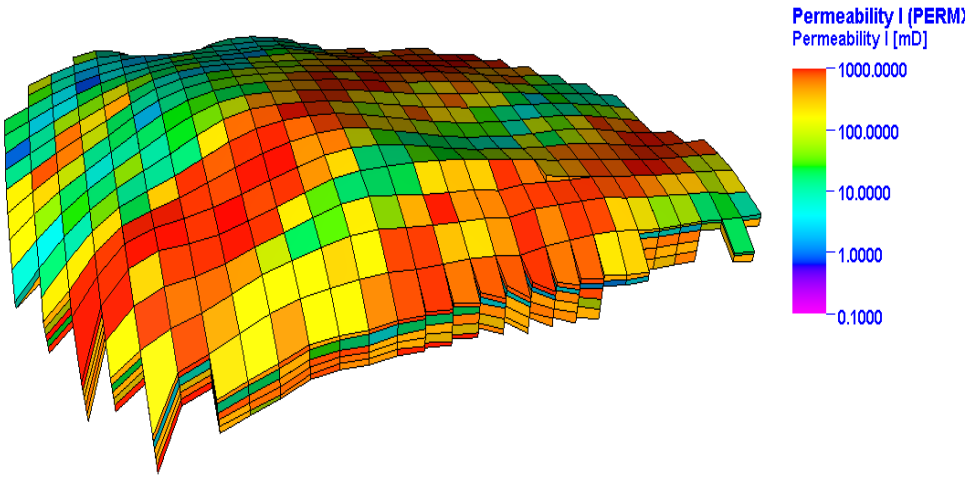

Figure 1. Horizontal permeability distribution.

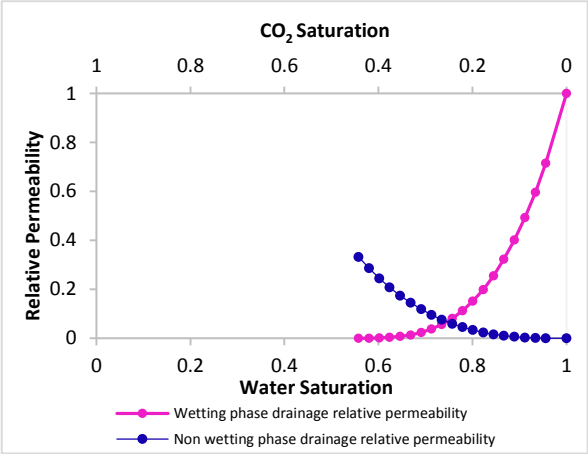

Figure 2. Relative permeability function of CO_2-H_2O system of Viking Sandstone.

Table 1. Basic input parameters for static modeling.

Parameter	Value	Parameter	Value
Irreducible water saturation	0.558	Average porosity	20%
Residual gas saturation	0.442	Average permeability	100 mD
Grid blocks	2660	Top depth	840 meter
Active cells	1760	Average reservoir thickness	15 meter
Length	180 meter	Initial pressure	300 bar
Width	180 meter	Initial temperature	90°C
Equilibrium Depth	2400 meter	Bottom hole pressure	400 bar
Overburden gradient	0.22 bar/meter	Phases	CO_2, H_2O & solid
Salt Precipitation	ON		

Table 2. Sensitivity cases and associated parameters.

Level	CASE A		CASE B		CASE C	
	Flow rate	$CaCO_3$	Flow rate	$CaCO_3$	Flow rate	$CaCO_3$
low	3×10^3	0.00	3×10^3	0.01	3×10^4	0.00
low	3×10^4	0.00	3×10^4	0.01	3×10^4	0.01
medium	3×10^5	0.00	3×10^5	0.01	3×10^4	0.02
high	3×10^6	0.00	3×10^6	0.01	3×10^7	0.00
high	3×10^7	0.00	3×10^7	0.01	3×10^7	0.01
high	3×10^8	0.00	3×10^8	0.01	3×10^7	0.02

[a]Components concentration in mole fraction

[b]Flow rate in sm^3/day

Table 3. Initial concentration of different components (0.90 H_2O and 0 CO_2).

CASE A			CASE B			CASE C		
NaCl	**$CaCl_2$**	**$CaCO_3$**	**NaCl**	**$CaCl_2$**	**$CaCO_3$**	**NaCl**	**$CaCl_2$**	**$CaCO_3$**
0.075	0.025	0.00	0.075	0.015	0.01	0.075	0.025	0.00
0.075	0.025	0.00	0.075	0.015	0.01	0.075	0.015	0.01
0.075	0.025	0.00	0.075	0.015	0.01	0.070	0.010	0.02
0.075	0.025	0.00	0.075	0.015	0.01	0.075	0.025	0.00
0.075	0.025	0.00	0.075	0.015	0.01	0.075	0.015	0.01
0.075	0.025	0.00	0.075	0.015	0.01	0.070	0.010	0.02

3. Results

The results obtained are presented in terms of amount and speed of free, residual and dissolved gases as a function of flow rate and $CaCO_3$ in three cases (i.e., A, B and C).

3.1 Effect of flow rate (Case A)

In this section, the effect of flow rate on trapping mechanisms in absence of $CaCO_3$ is discussed. The results of simulations for Case A are plotted against time at different flow rates as ploted in figure 3. As it is seen in this figure, increase of flow rate changes the amount of free CO_2 (structural trapping). It is noted that there is a linear relationship between the amount of free gas and flow rate for up to 10 to 20 years depending on injection rates. This relationship, howevere, starts to decline after 20 years due to rapid and continuous pressure buildup. Figure 4 shows the relationship between injection rate and immobile CO_2 in the model.

Showing in figure 4, there is a linear relationship between injection rate and immobile CO_2 (residual trapping) which is aligned with the findings of studies presented in the recent years [17-19]. This relationship is, however, significant only at medium and high injection rates (i.e., 3×10^5 and 3×10^6). In terms of residual trapping though, a similar trend is observed at high injection rates which increases rapidly up to 10 years and then becomes almost constant. This indicates that handling the flow rate would be useful to optimize the capillary trapping.

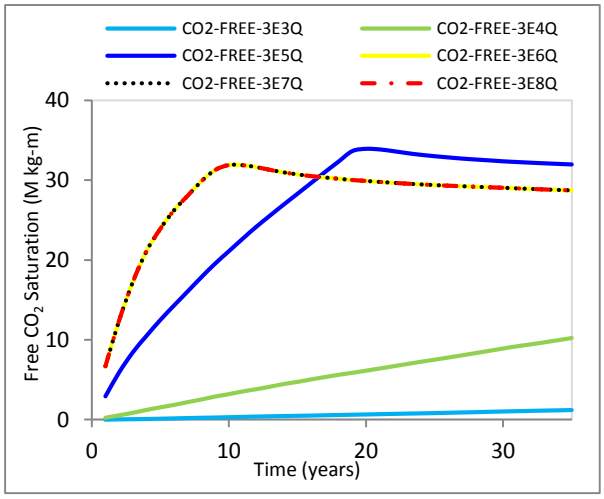

Figure 3. Effect of injection rate on free CO_2 saturation (Case A).

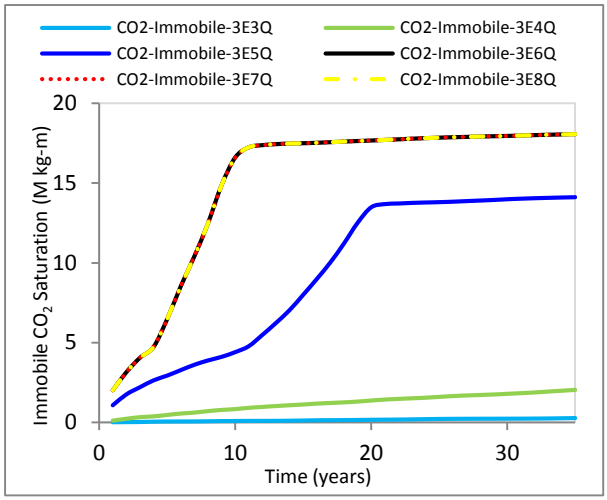

Figure 4. Effect of injection rate on immobile CO_2 saturation (Case A).

Variation of injection rates on the amount of dissolved gas (dissolution trapping) revealed a very same trend for free and immobile CO_2, as shown in figure 5. In fact, there is a rapid increase in CO_2 dissolution at medium and high injection rates immediately after injection begins, which is probably linked to dissolution kinetic factors [8]. The increase in solubility of CO_2 during continuous injection can also be attributed to pressure build up during the injection [21]. It is worth mentioning that the difference in the amount of dissolved CO_2 becomes smaller at medium and high injection rates. Figure 6 compares the trends obtained between trapping mechanisms and low injection rate (i.e., 3×10^3).

The results obtained from such comparison indicated that reservoir pressure builds up linearly during the injection period and structural trapping would be dominant at that stage. This means that low injection rate is not favorable for residual trapping and it may increase the risk of losing cap rock integrity due to long term exposure to free CO_2. A similar conclusion was made by Zhang and Song. (2014) as they indicated that structural and stratigraphic trappings are significant at low injection rate. Figure 7 compares the trends obtained between trapping mechanisms and high injection rate (i.e., 3×10^7).

The results obtained from curves included in figure 7 indicate that dissolved trapping is much significant than residual trapping. It can be concluded that high injection rate favors dissolution kinetic factor and suppress the capillary forces. It is important to note that free gas starts to decline after 10 years onwards at high injection rate when reservoir pressure becomes constant.

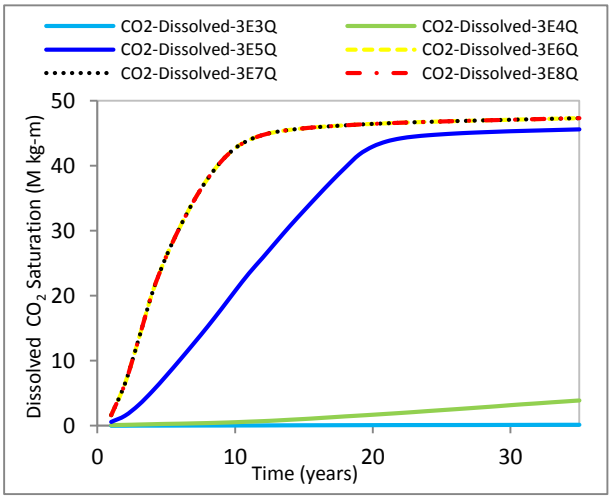

Figure 5. Effect of injection rate on dissolved CO_2 saturation (Case A).

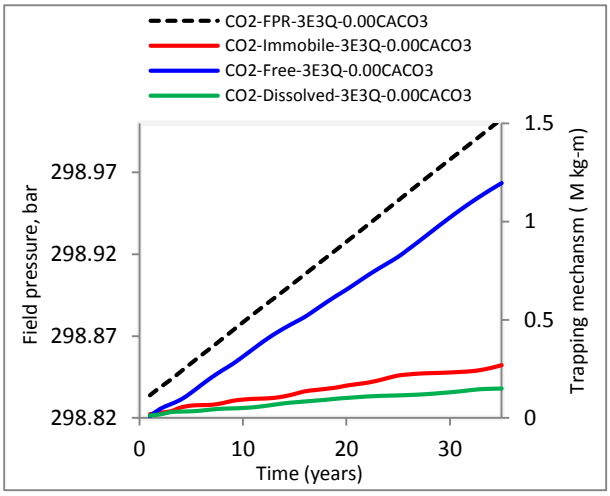

Figure 6. Comparison of trapping mechanisms at lower injection rate (Case A).

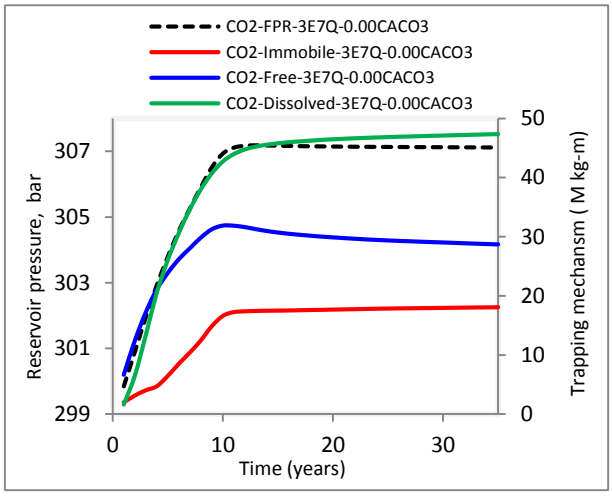

Figure 7. Comparison of trapping mechanisms at high injection rate (Case A).

3.2 Effect of flow rate in the presence of $CaCO_3$ (Case B)

In this section, the effect of flow rate on trapping mechanisms in presence of $CaCO_3$ is discussed. The results obtained for case B are presented in figures 8 to 10. No major impact is observed at low injection rates while trapping at high injection rates is significant. A very same analysis is done for Case B to evaluate the trends of free, residual and dissolution trapping mechanisms at low and high injection rates. The results obtained indicate that presence of $CaCO_3$ component in sandstone is offering more CO_2 entrapment during injection period (35 years) at medium and high injection rates as summarized in table 4.

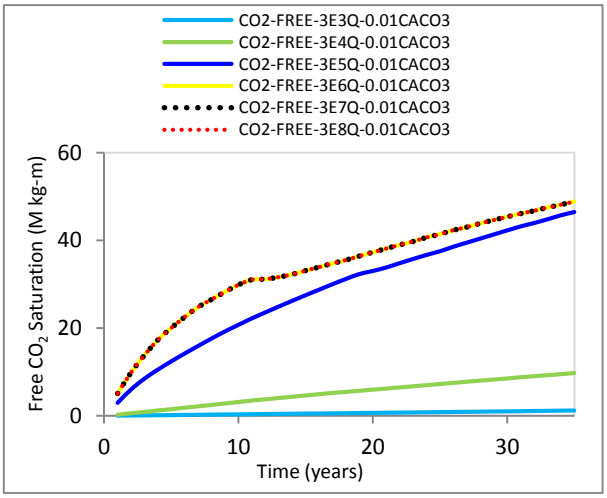

Figure 8. Effect of injection rate on free CO_2 saturation (Case B).

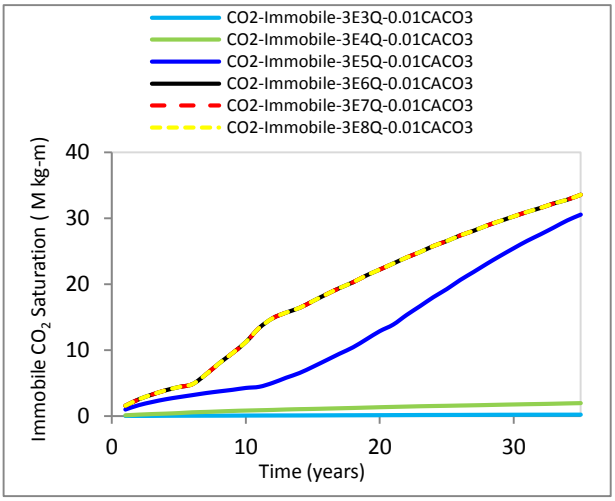

Figure 9. Effect of injection rate on immobile CO_2 saturation (Case B).

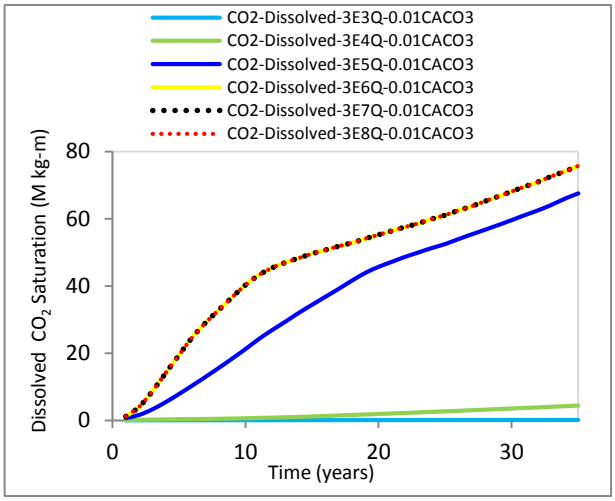

Figure 10. Effect of injection rate on dissolved CO_2 saturation (Case B).

Table 4. Comparison of trapping mechanisms efficiency with and without $CaCO_3$ component effect.

Flow rate, sm^3/D	Structural Trapping (M kg-m)		Residual Trapping (M kg-m)		Dissolution Trapping (M kg-m)	
	0.00 $CaCO_3$	*0.01 $CaCO_3$*	*0.00 $CaCO_3$*	*0.01 $CaCO_3$*	*0.00 $CaCO_3$*	*0.01 $CaCO_3$*
3×10^3	1.20	1.10	0.26	0.24	0.16	0.15
3×10^4	10.20	9.70	2.00	2.00	4.41	3.88
3×10^5	31.90	46.40	14.10	30.50	45.60	67.50
3×10^6	28.70	48.80	18.00	33.50	47.34	75.70
3×10^7	28.70	48.80	18.00	33.50	47.34	75.70
3×10^8	28.70	48.80	18.00	33.50	47.34	75.70

*Concentration is given in mole fraction

3.3 Effect of $CaCO_3$ (Case C)

In the last part of the study, the effect of $CaCO_3$ concentration on the trapping mechanisms is evaluated and discussed. Three $CaCO_3$ concentrations (i.e., 0.0 0, 0.01 and 0.02) are considered for the purpose of this study to evaluate their impacts on the trapping mechanisms. The results obtained are shown in figures 11 to 13.

The trend in figure 11 shows that there is no significant effect of $CaCO_3$ concentration on the free gas amount (structural trapping) at low injection rate (3×10^4). On the contrary, this impact is remarkable at high injection rate (3×10^7). Similar observation is made for the effect of $CaCO_3$ concentration on the amount of immobile (residual trapping) and dissolved CO_2 (dissolution trapping) as showing in figures 12 and 13. It is generally concluded that these relationships are not straightforward at early stages but will become directly proportional during the injection period. This might be due to time-dependent effect induced by $CaCO_3$.

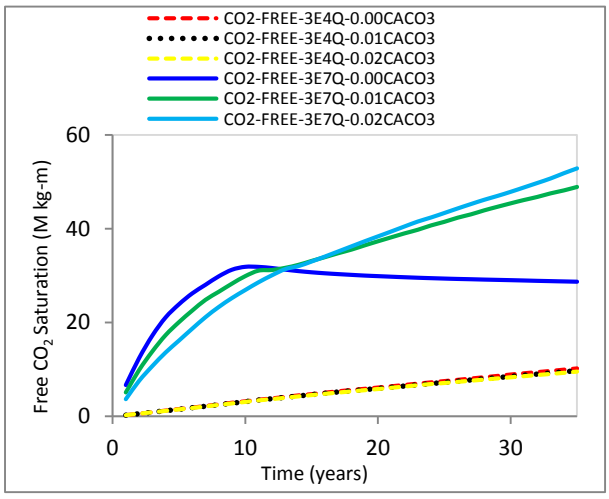

Figure 11. Comparison for the effect of $CACO_3$ component on free CO_2 saturation at 3E4 and 3E7 injection rates (Case C).

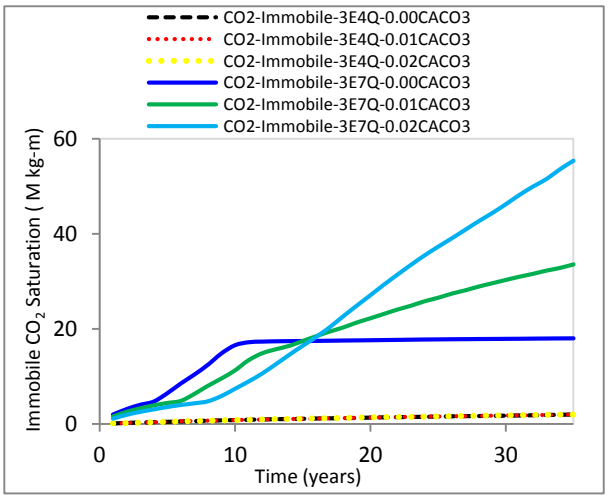

Figure 12. Comparison for the effect of $CACO_3$ component on immobile CO_2 saturation at 3E4 and 3E7 injection rates (Case C).

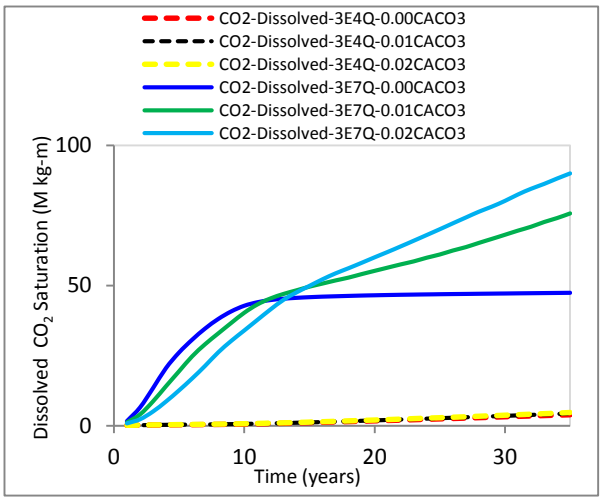

Figure 13. Comparison for the effect of $CACO_3$ component on dissolved CO_2 saturation at 3E4 and 3E7 injection rates (Case C).

4. Conclusions

In this study attempts are made to evaluate the effect of injection rate and $CaCO_3$ concentration on trapping mechanisms of heterogeneous aquifers. The results obtained reveal that selection of injection rate is important to get the highest capacity of a storage medium for CO_2 entrapment. This study also reveals that there is a direct relationship between flow rate and trapping mechanism at very low injection rates. The sequence of trapping mechanisms is also dependent on the level of injection rate. The injection rate is directly linked to the trapping mechanisms when $CaCO_3$ concentration is included in the analysis. The presence of $CaCO_3$ doesn't have any significant impact on the trapping at low injection rates but this effect might have been significant at high injection rate.

References

[1]. Akintunde O, Knapp C and Knapp J 2013 Petrophysical characterization of the south georgia rift basin for supercritical CO_2 storage: A preliminary assessment *Environmental Earth Sciences.* **70**(7): p. 2971-2985.
[2]. Zhao B, MacMinn W C and Juanes R 2014 Residual trapping, solubility trapping and capillary pinning complement each other to limit CO_2 migration in deep saline aquifers *Energy Procedia*. **63**: p. 3833-3839.
[3]. Espie A 2005 CO_2 capture and storage: contributing to sustainable world growth *International Petroleum Technology Conference*.
[4]. Iglauer S, Paluszny A, Pentland C H and Blunt M J 2011 Residual CO_2 imaged with x-ray micro-tomography *Geophysical Research Letters*. **38**(21).
[5]. Juanes R, Spiteri E, Orr F and Blunt M 2006 Impact of relative permeability hysteresis on geological CO_2 storage *Water Resources Research.* **42**(12).
[6]. Taku Ide S, Jessen K and Orr Jr F M 2007 Storage of CO_2 in saline aquifers: Effects of gravity, viscous, and capillary forces on amount and timing of trapping *International Journal of Greenhouse Gas Control*. **1**(4): p. 481-491.
[7]. Benson S M and Cole D R 2008 CO_2 sequestration in deep sedimentary formations *Elements*. **4**(5): p. 325-331.
[8]. Zhang D and Song J 2014 Mechanisms for geological carbon sequestration *Procedia IUTAM*. **10**(0): p. 319-327.
[9]. Saeedi A 2012 Experimental study of multiphase flow in porous media during CO_2 geo-sequestration processes *Springer Science & Business Media*.

[10]. Pentland C H, El-Maghraby R, Iglauer S and Blunt M J 2011 Measurements of the capillary trapping of super-critical carbon dioxide in Berea sandstone *Geophysical Research Letters*. **38**(6).
[11]. Iglauer S 2011 *Dissolution Trapping of Carbon Dioxide in Reservoir Formation Brine-A Carbon Storage Mechanism.* In: Mass Transfer (ed.: Nakajima H), ijeka.
[12]. Ketzer J M, Iglesias R and Einloft S 2012 *Reducing Greenhouse Gas Emissions with CO_2 Capture and Geological Storage* in Handbook of Climate Change Mitigation, W.-Y. Chen, et al., Editors, Springer US. p. 1405-1440.
[13]. Raza A, Rezaee R, Bing C H, Gholami R, Hamid M A and Nagarajan R 2016 Carbon dioxide storage in subsurface geologic medium: A review on capillary trapping mechanism *Egyptian Journal of Petroleum (EGYJP)-Elsevier (in press)*.
[14]. Solomon S 2006 Criteria for intermediate storage of carbon dioxide in geological formations *The Bellona Foundation*, Oslo.
[15]. Kimbrel E H, Herring A L, Armstrong R T, Lunati I, Bay B K and Wildenschild D 2015 Experimental characterization of nonwetting phase trapping and implications for geologic CO_2 sequestration *International Journal of Greenhouse Gas Control*. V**42**: p. 1-15.
[16]. Blunt M J and Scher H 1995 Pore-level modeling of wetting *Physical Review* E. **52**(6): p. 6387.
[17]. Nguyen V H, Sheppard A P, Knackstedt M A and Pinczewski W V 2006 The effect of displacement rate on imbibition relative permeability and residual saturation *Journal of Petroleum Science and Engineering*. **52**(1): p. 54-70.
[18]. Wildenschild D, Armstrong R T, Herring A L, Young I M and Carey J W 2011 Exploring capillary trapping efficiency as a function of interfacial tension, viscosity, and flow rate *Energy Procedia*. V**4**: **p.** 4945-4952.
[19]. Soroush M, Wessel-Berg D, Torsaeter O and Kleppe J 2013 Investigating impact of flow rate and wettability on residual trapping in CO_2 storage in saline aquifers through relative permeability experiments *Energy and Environment Research*. **3**(2): p.53.
[20]. Schlumberger 2014, Technical Description 2014.2.
[21]. Bahadori A, Vuthaluru H B and Mokhatab S 2009 New correlations predict aqueous solubility and density of carbon dioxide *International Journal of Greenhouse Gas Control*. **3**(4): p. 474-480.

Acknowledgments
This work was funded by Curtin University Sarawak Malaysia through the Curtin Sarawak Research Institute (CSRI) Flagship scheme. We used the relative permeability CO_2-H_2O data available at Alberta Geological Survey (AGS) and static modeling data from Juanes Research Group (JRG), Massachusetts Institute of Technology. Schlumberger Malaysia is also acknowledged for the Petrel tool and Eclipse Reservoir Simulator licenses.